Resource Mapping at Tidal Energy Sites

Michael Palodichuk, Brian Polagye, and Jim Thomson

***Abstract*—Station keeping, a vessel-based spatial surveying method for resolving details of the hydrokinetic resource, is presented in the context of the general methodology and also for the specific case of a survey conducted in northern Admiralty Inlet, Puget Sound, WA, in June 2011. The acoustic Doppler current profiler (ADCP) measurements collected during the June 2011 survey were part of a broader effort to characterize the resource at this location before tidal turbine installation. Autonomous bottom-lander (bottom-mounted) ADCP measurements are used to evaluate the accuracy with which data collected from this vessel-based survey reflect stationary measurements and also to analyze the potential for cycle-to-cycle variations in the conclusions drawn. Results indicate good agreement between shipboard and bottom-mounted observations in capturing spatial resource differences. Repeated surveys over several tidal cycles are required to obtain results consistent with long-term observations. Station-keeping surveys help to optimize bottom-mounted ADCP deployments that are then used to estimate turbine power generation potential and make final siting decisions.**

***Index Terms*—Acoustic Doppler current profiler (ADCP), marine and hydrokinetic energy, micrositing, oceanographic techniques, shipboard surveys, tidal energy, tidal power.**

I. Introduction

TIDAL hydrokinetic energy is harnessed by free-stream turbines that convert the kinetic energy of strong (>1 m/s) tidal currents to electricity. Project economics are improved by siting these turbines where the hydrokinetic resource is most energetic and resource characterization is a typical early stage project development activity. Robust estimates for the long-term power generation potential of a site require a current observation of at least 30 days [1]. When resource variations are small within the region of survey interest, a single, autonomous Doppler profiler deployment can provide suitable information. However, when operationally significant differences in the kinetic resource (i.e., 5%–10% variations in mean power generation) occur over length scales as short as 100 m, selecting an optimal deployment location *a priori* may not be possible [1]. In these cases, resource differences can be resolved through multiple deployments of autonomous profilers, but identifying local maxima in resource intensity may be both time consuming and expensive. Therefore, it is desirable to develop low-cost ship-mounted Doppler profiler surveys that can resolve resource differences over length scales $O(100\text{ m})$ and optimize bottom-lander target selection.

Manuscript received March 15, 2012; revised October 07, 2012; accepted November 01, 2012. Date of publication January 22, 2013; date of current version July 10, 2013. This paper was supported by the U.S. Department of Energy and the Snohomish County Public Utility District. Neither the United States Government nor any agency thereof, nor any of their employees, makes any warranty, expressed or implied, or assumes any legal liability or responsibility for the accuracy, completeness, or usefulness of any information, apparatus, product, or process disclosed, or represents that is use would not infringe privately owned rights. Reference herein to any specific commercial product, process, or service by trade name, trademark, manufacturer, or otherwise does not necessarily constitute or imply its endorsement, recommendation, or favoring by the U.S. Government or any agency thereof. Their views and opinions of the authors expressed herein do not necessarily state or reflect those of the U.S. Government or any agency thereof.

Associate Editor: H. Maeda.

The authors are with the Northwest National Marine Renewable Energy Center, University of Washington, Seattle, WA 98195 USA (e-mail: mpalod@u.washington.edu).

Digital Object Identifier 10.1109/JOE.2012.2227578

A. Literature Review

The potential for ship-mounted acoustic Doppler current profiler (ADCP) surveys to resolve tidal current variations was demonstrated by Simpson *et al.* [2], where they attempted to de-tide observed currents (i.e., removing tidal currents). Repeated transects across a 20-km channel between Scotland and Herbides (the Minch) were conducted for approximately one semidiurnal period on two separate cruises and used to map the flow through the Minch into volumetric bins (i.e., a 3-D grid). A compound space–time series of measurements at each bin was built up through repeated surveys, and least squares tidal harmonic analysis was performed to estimate the primary semidiurnal tidal constituents at these discrete points in the profiling transect (1500-m horizontal resolution). The M2 amplitude and phase were in general agreement with a model by Proctor and Wolfe [3]. A similar repeated transect methodology was employed by Geyer and Signell [4] to obtain the spatial structure of tidal flow around a headland in Vineyard Sound, MA. Five 10-km trapezoidal tracks with overlapping edges were surveyed over eight cruises. The semidiurnal amplitude was normalized by moored current meter data, and consistency was shown among the different cruises. The measurements from the separate cruises were merged to form a composite spatial representation of current variations (up to 500-m horizontal resolution). Vennell [5] applied the method developed by Simpson *et al.* to Cook Strait, New Zealand, to determine the horizontal and vertical variation of tidal phase and amplitude within the Strait for a single observed tidal cycle (2500-m horizontal resolution). The measured semidiurnal tidal amplitude and phase agreed well with a hindcast composite of the three largest tidal constituents from a subsequent one month deployment of bottom-lander ADCPs on the same line as the ship track [6].

For surveys with greater spatial extent, Candela *et al.* [7] developed a methodology that requires only a single survey spanning multiple diurnal periods with no repetitions of any transect. This methodology was applied in the Yellow Sea on a five-day cruise over a total survey area of 300 km $\times$ 500 km, with 20-km horizontal bins along the ship's track. The primary diurnal and semidiurnal constituents amplitudes and phases were described as functions of spatial position, and the tidal spatial structure was approximated using arbitrary interpolating base functions. These spatial base functions simulated the horizontal distribution of tidal properties, and their coefficients were set to minimize the residual between observations and the model. Foreman and Freeland [8] followed a similar data collection procedure on a three-day cruise around Vancouver Island, Canada, and found that detiding observations using a barotropic numerical model performed better than prescribing spatial base functions.

To demonstrate the physical soundness and consistency of obtained tidal data and subtidal velocity estimates in the mouth of Delaware Bay, Münchow *et al.* [9] applied both the repeated transect with harmonic analysis method and the spatial base function method to remove tidal currents, as well as a third method where nearby current meters were used to interpolate tidal currents to the measurement locations. Each discrete station corresponded to a spatial average along the ship track of almost 1000 m, and close agreement of subtidal velocity structure was found among the three methods. Data collection methods similar to the repeated transect method have been employed by Cáceres *et al.* [10] in Chacao Channel, Southern Chile and Stevens *et al.* [11] in Cook Strait, New Zealand. Vennell and Beatson [12] replaced the volumetric box binning technique with radial basis functions to improve the tidal velocity field extracted from noisy shipboard measurements collected in Bluff Harbour, New Zealand at spatial scales $O(100\text{ m})$.

Each of these approaches could conceivably be modified to resolve hydrokinetic resource variations, but not without difficulty. Most of the techniques involving repeated transits or circuits [2], [4], [6], [9]–[11] would require at least 25 h of survey effort in mixed tidal regimes (these techniques were all applied to dominantly semidiurnal sites). Further, these provide information about the harmonic constituents, which may not constitute a complete representation of current velocity at tidal energy sites [13]. Those techniques that involve a single transit through a survey area require a validated numerical model for effective detiding [7], [8], in which case, hydrokinetic resource variations could be estimated directly from the model without the expense of a survey. However, validated $O(100\text{ m})$ resolution models of tidal energy sites are rare.

An example of a prior method adapted to micrositing of tidal turbines in mixed tidal regimes is presented by Epler *et al.* [14], who demonstrated a "racetrack" survey involving repeated short tracks encompassing a single tidal peak. As in [2], data were aggregated into bins (100-m horizontal resolution) to produce a space–time series of currents as a function of horizontal and vertical positions. For each bin, the time series was then fitted with a half-sine-wave, and the amplitude and timing of the peak currents along the survey track were estimated from the fit. This technique was applied to Admiralty Inlet, Puget Sound, WA, and used to resolve strong resource differences (i.e., variations in peak tidal current magnitude of at least 0.3 m/s). However, the effectiveness of this technique likely depends on an implicit filtering of turbulence via the half-sine-wave fit (i.e., each bin is occupied for 1 min or less; over this time scale turbulence may significantly increase or reduce measured currents relative to mean flow conditions [15]).

TABLE I
SHIPBOARD ADCP CONFIGURATION

Teledyne RDI Workhorse Monitor	
Acoustical Frequency	307.2 kHz
Time per Ping	0.5 s
Time between Pings	1 - 2 s
Vertical Bin Size	4.0 m
Pings / Ensemble	1
Doppler Uncertainty	0.05 m/s
Transducer Depth	1.0 m
Blanking Distance	2.0 m
Motion Compensation	Bottom Tracking

B. Overview

A "station-keeping" vessel-based survey methodology was developed in this study to resolve small spatial scale differences in the hydrokinetic resource at low cost. During a station-keeping survey, a vessel occupies each target stations for several short periods bracketing a single tidal peak. This is unlike the continuous transect surveys previously described. Here, uncertainty in each observation is minimized by averaging out variability associated with turbulent fluctuations and, thus, capturing only information about the deterministic component of the currents. Additionally, a kinetic energy metric is computed and used to compare the hydrokinetic resource among the surveyed stations, rather than defining resource differences in terms of velocity variations. Information about peak tidal current magnitude variations is not as useful as information about kinetic energy variations, since the former is not directly correlated with power generation potential from a tidal turbine, but the latter is.

In this paper, the vessel-based station-keeping methodology is presented and an application to a specific site is described. The data sets and their usage are introduced in Section II-A. They include:

- shipboard data set: temporally sparse observations collected from a surface vessel to demonstrate the station-keeping methodology to resolve spatial resource variations;
- bottom-mounted data set: continuous observations from bottom-mounted profilers to ground truth the accuracy of aspects of the station-keeping methodology;
- decimated bottom-mounted data set: temporally sparse, long-term observations to determine the effectiveness of this technique to resolve spatial resource variations in the long-term average hydrokinetic resource (i.e., average calculated over 30 days or longer).

The station-keeping procedure, data processing techniques, and means for station comparison are outlined in Sections II-B–II-D. Results from the June 2011 station-keeping survey in Admiralty Inlet are then presented in Section III. The effectiveness of this methodology to accurately resolve long-term average spatial variations in the hydrokinetic resource and accuracy of the survey technique are discussed in Section IV.

II. METHODOLOGY

Northern Admiralty Inlet, the main entrance to the Puget Sound, has been identified as a favorable site for tidal energy development, since the tidal exchange through the relative

TABLE II
SUMMARY OF SURVEY STATIONS FOR JUNE 2011 SURVEY AND BOTTOM-MOUNTED ADCP CONFIGURATIONS AND DEPLOYMENTS

Station	Distance to Station A (m)	Bottom-Mount ADCP Site	Distance from Station to Bottom-Mount ADCP Site (m)	Bottom-Mount Instrument	Bottom-Mount Deployment Dates (dd/mm/yy)	Duration (days)	Mean Depth (m)
A	0	1	2	Nortek Continental 470 kHz	18/08/10 - 09/08/11	356	59
B	52	2	16	Nortek AWAC[1] 600 kHz	11/05/11 - 09/08/11	90	61
C	238	3	7	Nortek AWAC[1] 1 MHz	09/05/11 - 08/06/11	30	56
D	145	None	N/A	N/A	N/A	N/A	No Data
E	117	None	N/A	N/A	N/A	N/A	No Data

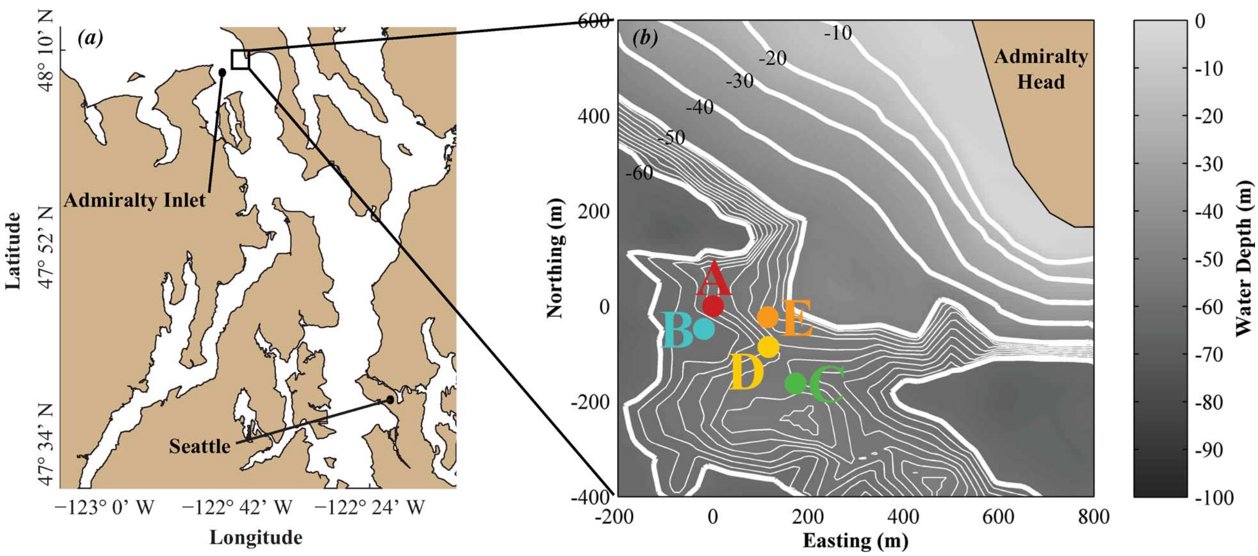

Fig. 1. Admiralty Inlet tidal energy project area. (a) Regional map. (b) June 2011 station-keeping survey stations overlaying bathymetry (1-m contours are shown for depths between 50 and 60 m).

constriction of the channel cross section gives rise to strong currents. A hydrokinetic pilot project has been proposed at this location, undertaken by Snohomish County Public Utility District (Everett, WA) and OpenHydro, Ltd (County Louth, Ireland). A multiyear field study was conducted to broadly characterize the resource before tidal turbine installation. Current measurements, collected using ADCPs, were a component of these studies. This section describes both the general methodology for a station-keeping survey and the specific case for a station-keeping survey conducted in northern Admiralty Inlet.

A. Data Sets Synopsis

Tidal currents were measured by ADCPs, which use active acoustics to measure currents throughout the water column.[1] In this study, two types of ADCP data sets were analyzed—those collected from a surface vessel ("shipboard") and those collected from an autonomous bottom lander ("bottom-mounted"). The station-keeping methodology required only shipboard data. The bottom-mounted data set was used as "truth" to evaluate the accuracy with which data collected from a quasi-stationary surface vessel reflected a stationary measurement and also to mimic station-keeping surveys over multiple tidal cycles.

1) Shipboard Data Set: Shipboard surveys were conducted from the University of Washington's Applied Physics Laboratory Research Vessel Jack Robertson (*R/V Jack Robertson*). Current velocity data were collected using a through-hull Teledyne RDI Workhorse Monitor with instrument configuration given in Table I. The shipboard ADCP data consisted of repeated, short (5 min) observations during which the vessel occupied a target station. As discussed in Section IV-C, the 5-min temporal mean filtered the majority of turbulence from the measured velocity and limited Doppler uncertainty. The data collection procedure is explained in detail in Section II-B.

In June 2011, a station-keeping survey with five target stations was conducted in Admiralty Inlet. The target stations are summarized in Table II and shown in Fig. 1. Station-keeping targets A, B, and C were selected to be cospatial with bottom-mounted ADCPs deployed during a prior research cruise. Stations D and E were of potential interest as alternative siting locations for the turbines. All of these stations had acceptable slope, depth, and seabed conditions to be considered for turbine deployment. Station A was used as the reference location

[1]ADCP is a common term from the manufacturer Teledyne RDI (Poway, CA). The acoustic wave and current meter (AWAC) is a similar instrument from Nortek (Oslo, Norway).

throughout this study. The June 2011 survey was conducted during an ebb tide in the transitional period between neap and spring tides with peak current velocities around 2 m/s.

2) Bottom-Mounted Data Set: The objective of this study was to demonstrate the suitability of station keeping, a self-contained shipboard methodology, to resolve difference in the hydrokinetic resource to optimize long-term bottom-mounted deployments suitable for power generation estimates. Bottom-mounted data sets were used to achieve two objectives. First, they served to evaluate the accuracy of station keeping relative to stationary "truth" at survey locations by direct comparison of bottom-mounted and station-keeping time series. Second, effectiveness of this technique to resolve long-term average resource variations was evaluated by mimicking multiple station-keeping surveys during different tidal cycles (e.g., spring/neap, ebb/flood, greater/lesser).

As described in [1], bottom-mounted ADCPs were deployed in an upward-looking configuration on ballasted fiberglass tripods (Oceanscience Sea Spiders) for periods of up to three months. The instrument head was approximately 0.7 m above the seabed and the blanking distance varied from 0.4 to 1.0 m. Sea Spiders were lowered to the seabed and as-deployed locations recorded by the Differential Global Positioning System (DGPS). Wire angles were minimized by drifting during deployments, and recovery positions were typically within 5 m of as-deployed locations (i.e., within DGPS error). Details of each deployment are given in Table II and shown in Fig. 1. Bottom-mounted site 1 was a composite record consisting of four deployments, each approximately three months in duration from within a 20-m radius. In the context of this study, bottom-mounted site 1 is referred to as the "annual data set."

3) Decimated Data Set: Each bottom-mounted ADCP provided continuous, long-term time-series observations for a station. In a vessel-based, station-keeping survey, each station was occupied for several short periods. For example, in the June 2011 survey, each station was occupied six times for 5 min, with each observation of an individual station separated by 30–40 min. To evaluate the ability of the station-keeping methodology to resolve long-term average resource variations, bottom-mounted data from 30+ day deployments were decimated to mimic shipboard data.

To create these data sets, the raw, 1-min ensembles from bottom-mounted ADCPs were first averaged to 5-min ensembles and separated into individual ebb or flood cycles. As with shipboard ADCP data, bottom-mounted ADCP data were influenced by turbulence and Doppler uncertainty. The 5-min temporal mean minimized theses effects (Section IV-C) and mimicked the observations that would have been collected during a station-keeping survey. To simulate a survey pattern, six sequential ensembles, each separated by 35 min, were selected. Survey start time was incremented to simulate variations in observation timing relative to peak currents, yielding 20 survey realizations per tidal cycle. For reasons described in Section IV-C, only realizations from cycles with peak currents exceeding 1 m/s, durations of at least 4.5 h, and at least 2.25 h between slack water and peak currents were retained. Hereafter, the collection of all realizations meeting these restrictions is referred to as the "decimated data set."

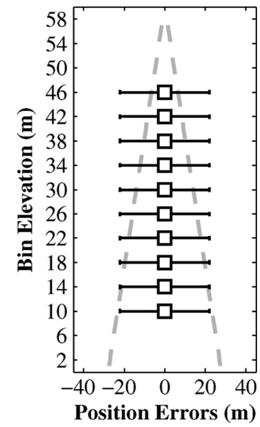

Fig. 2. Position errors throughout the water column. Horizontal bars denote the vessel's typical track error while holding station over the target, and dashed lines denote beam spread of the shipboard ADCP.

Comparisons between shipboard and bottom-mounted data are presented at 22-m elevation relative to the seabed throughout this paper. This was a depth within the range of both shipboard and bottom-mounted observations, was within the range of hub heights for first generation tidal turbines, and was outside the region of strongest vertical shear near the seabed.

B. Procedure for a Station-Keeping Survey

Observations from a station-keeping survey were collected around the time of peak currents since these provide the strongest signal for resolving spatial variations and also represent the period of maximum power output from a hydrokinetic tidal turbine (kinetic resource intensity varies with the cube of velocity). During a station-keeping survey, the survey vessel sequentially occupied the target stations to obtain a sparse time series for each station, ideally with an equal number of observations to either side of peak currents.

Sections II-B1–II-B4 present the temporal resolution, spatial resolution, observation timing, and tidal conditions recommended for this survey technique. The justifications for these recommendations are described in detail in Section IV-C.

1) Temporal Resolution: Each observation at a station needed to be sufficiently long to capture only information about mean currents (as opposed to turbulent fluctuations). However, the observations needed to be sufficiently short such that the mean currents were stationary. For Admiralty Inlet, Thomson *et al.* [15] suggested that a 5-min ensemble average could achieve these objectives. Additionally, Doppler uncertainty in the ensemble average for an observation needed to be sufficiently low to avoid biasing the results. Measurement precision depends upon the frequency of the Doppler profiler, bin size, and number of pings per ensemble. For tidal energy sites, such as the one described in this paper, velocity measurement precision better than 0.05 m/s generally required $O(100$ pings/observation) (Section IV-C).

2) Spatial Resolution: In a station-keeping survey, observations were not made at a single point. Rather, vessel, DGPS uncertainty, and Doppler profiler beam spread resulted in a region of ambiguity for measurements at a nominal target station, as shown in Fig. 2. The track (i.e., vessel movement), DGPS, and beam spread errors were uncorrelated and were combined using

(1) to obtain a total position error δ_r with respect to the target station. In order for observations between two stations to be statistically independent, the position ambiguities (i.e., target location $\pm\delta_r$) were not to overlap. Independence between two stations was tested by (2)

$$\delta_r = \sqrt{\delta^2_{\mathrm{track}} + \delta^2_{\mathrm{DGPS}} + \delta^2_{\mathrm{beam}}} \tag{1}$$

$$\sqrt{(x_1 - x_2)^2 + (y_1 - y_2)^2} - \delta_{r1} - \delta_{r2} > 0. \tag{2}$$

3) Observation Timing: The number of and relative separation between target stations influenced the number of observations that could be collected per station and the time interval between each observation. The error associated with this station-keeping methodology was minimized for surveys with at least five observations per station and 30–40-min intervals between observations at an individual station (Section IV-C). Errors were further minimized for surveys with an equal number of observations to either side of peak currents (Section IV-C).

4) Tidal Conditions: Surveys needed to be conducted during tidal cycles that have sufficient time for observations (including an allowance for uncertainty in the timing of peak currents) and provided strong signal for resolving spatial variations. For locations with mixed tidal regimes (i.e., significant diurnal variability), the effectiveness of station-keeping surveys was improved when they were performed during greater tides (Section IV-C).

C. Data Processing

For the vessel-mounted Doppler profiler, profiler motions were removed from measurements to obtain absolute water velocities using bottom tracking [16]. Hard returns from the seafloor contaminated measurements in the lowest bins. Measured values not meeting a minimum correlation count (e.g., 70) were removed. Any measurements from outside a defined vessel position tolerance radius for a target station were also discarded. The quality assured data were then processed in the following steps.

1) Ensemble-Average Velocity: The representative ensemble-average current velocity for each observation (u_{obs}) was calculated for each depth bin using

$$\begin{aligned} u_{\mathrm{obs}} = \overline{u_{\mathrm{meas}}} &= \overline{u_{\mathrm{det}} + u_{\mathrm{met}} + u_{\mathrm{turb}} \pm n_{\mathrm{samp}}} \\ &\approx u_{\mathrm{det}} + u_{\mathrm{met}} \pm n_{\mathrm{ens}}. \end{aligned} \tag{3}$$

The population mean and standard deviation of each observation was unknown and was estimated from the sample mean and standard deviation. There were sufficient pings per ensemble to assume a normal statistical distribution for turbulent perturbations and Doppler noise.

The temporal mean filtered the majority of the turbulent scale motion from the signal (u_{turb}) [15], while preserving the deterministic (u_{det}) and meteorological (u_{met}) components (further discussion in Section IV-C). Ensemble averaging also reduced the Doppler noise (η_{ens}) by a factor of $N^{1/2}$ relative to the Doppler noise in the raw measurement (η_{samp}), where N is the number of samples in the ensemble.

2) Kinetic Power Density: The power generated by a tidal turbine is proportional to the cube of the current velocity. Consequently, a kinetic power or energy metric was more appropriate for mapping resource variations than a velocity metric. Kinetic power density (K) was computed for each velocity observation as

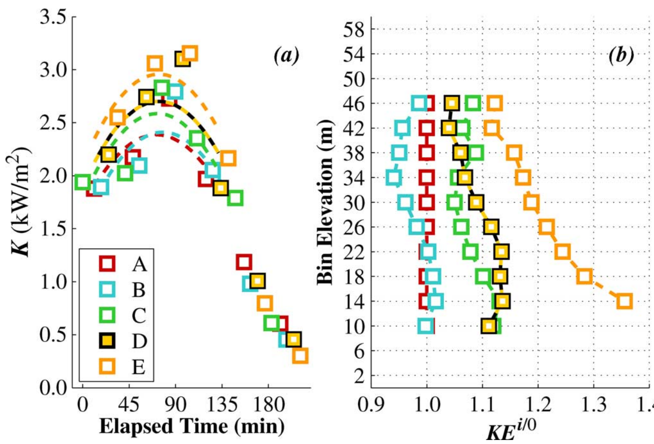

Fig. 3. Comparison of the hydrokinetic resource among target stations. (a) Polynomial curve fits through observed K at 22-m elevation relative to seabed. (b) Normalized KE values with respect to station A. Note that one of the six observations at station E contained contaminated data in the bottommost (10 m) bin; this data is not shown.

$$K = \frac{1}{2}\rho u^3_{\mathrm{obs}} \tag{4}$$

where ρ is density (assumed to be 1024 kg/m^3). This was not identical to the average of the kinetic power density for each ping in the ensemble (i.e., the mean of the cube was not equal to the cube of the mean). Doppler noise and turbulence intensity, assumed to have zero mean values and defined by their second moments, did not bias the mean velocity. However, if K were computed directly from each ping, the result would have been biased high by the symmetric variance in these systems (real for turbulence, measurement artifact for Doppler noise). To avoid a systematic error in kinetic power density computation from Doppler noise, the best unbiased velocity value was used (i.e., the ensemble mean). Based on analysis of high-resolution bottom-mounted data (i.e., 1-Hz single ping data), the difference between $\overline{u_{\mathrm{meas}}}^3$ and $\overline{u^3_{\mathrm{meas}}}$ was not significant for a 5-min ensemble at this location (not shown).

Because measurements of kinetic power density were sparse in a station-keeping survey and were obtained at each station at different times relative to the peak currents, resource differences derived from a single occupation of each station were likely subject to high uncertainty. Consequently, a representation of resource intensity was required that was insensitive to variations between locations at different times within a single tidal cycle (e.g., as could be caused by strong variations in the tidal current phase). A second-order polynomial was fit to the observations at a station in Matlab (www.mathworks.com) using the default unconstrained nonlinear optimization routine

$$\widetilde{K}(t) = x_0 + x_1 t + x_2 t^2 \tag{5}$$

where $\widetilde{K}$ is the empirical fit to the observations of K and x are the polynomial coefficients. The appropriateness of this empirical fit is discussed in an Appendix.

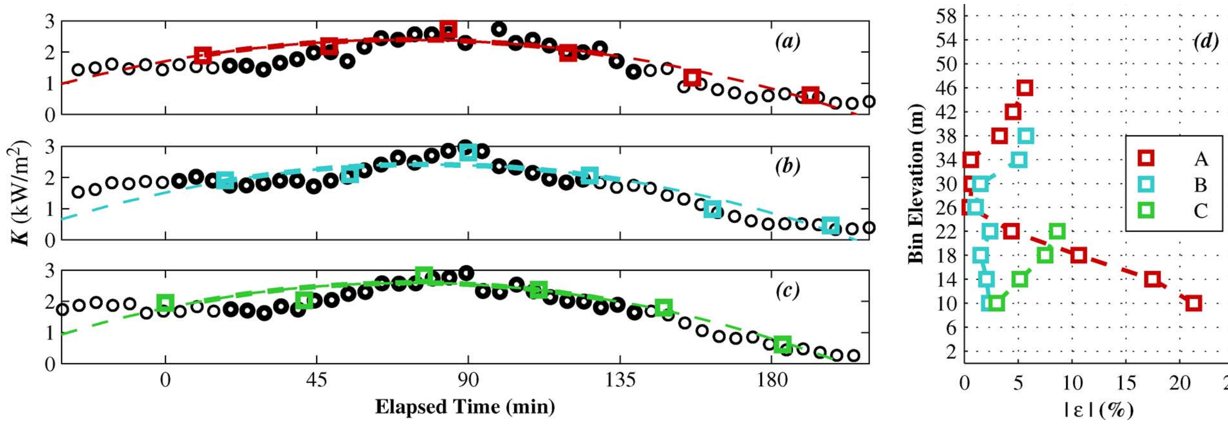

Fig. 4. Shipboard and bottom-mounted observations of K and KE. Comparison of observed K at 22-m elevation for (a) station A; (b) station B; and (c) station C (cospatial with sites 1–3, respectively). Circles denote bottom-mounted ensembles, with the bold circles used to compute the "true" KE. The dashed line denotes the fit to the shipboard ensemble (squares), with the bold portion used to compute the "observed" KE. (d) Relative error between the observed and true KE as a function of depth. Note that the comparison is only possible for common vertical bins between the two instruments: the upward-looking ADCPs have a maximum range set by their operating frequency. For example, the 1-MHz acoustical frequency of the bottom-mounted ADCP at station C limits its profiling range to 25 m. The downward-looking ADCP signal is contaminated by the hard return from the seabed in the lowest two bins.

TABLE III
NORMALIZED KINETIC ENERGY DENSITIES

Station	$KE^{i/0}$	
	Shipboard ("obs") [1]	Bottom-Mounted ("true") [2]
A ("0")	1.00 ± 0.14	1.00
B	1.00 ± 0.14	1.02
C	1.08 ± 0.15	1.03
D	1.13 ± 0.16	No Data
E	1.24 ± 0.17	No Data

[1] Standard error based on the analysis of decimated data set (Fig. 12)
[2] Bottom-mounted KE, sampled at a finer temporal resolution and calculated from data, rather than a polynomial approximation, has negligible errors in comparison to the vessel-based observations

3) Kinetic Energy Density: The kinetic energy density (KE) was obtained by numerically integrating $\widetilde{K}$ over a 2-h period using a cumulative trapezoidal method, the end points of which were iteratively selected to maximize the calculated KE. This was used to provide an estimate for relative resource intensity differences between stations that was insensitive to the times at which the stations were occupied. A 2-h window, chosen iteratively to maximize the kinetic energy within the window, was chosen (Section IV-C).

An estimate for the "true" KE for a tidal cycle was obtained from bottom-mounted data by numerically integrating the undecimated observations of K (again using a cumulative trapezoidal method). The relative error (ϵ) between the fit to observations (either shipboard or decimated bottom mount) and "truth" was evaluated using

$$\epsilon = \frac{KE_{\text{obs}} - KE_{\text{true}}}{KE_{\text{obs}}}. \tag{6}$$

The standard relative error (σ_ϵ) was defined as the standard deviation of the relative errors for all realizations in the decimated data set at site 1 (further discussion in Section IV-C).

D. Kinetic Energy Density Normalization

The objective of the station-keeping methodology was to resolve relative resource differences, not quantify the absolute resource variations between stations (that quantification requires long-term bottom-mounted data for high accuracy). The hydrokinetic resource was compared between two stations by normalizing their KE values to a reference

$$KE_{\text{obs}}^{\frac{i}{0}} = \frac{KE_{\text{obs}}^{i}}{KE_{\text{obs}}^{0}} \tag{7}$$

$$KE_{\text{true}}^{\frac{i}{0}} = \frac{KE_{\text{obs}}^{i}(1 \pm \sigma_\epsilon)}{KE_{\text{obs}}^{0}(1 \pm \sigma_\epsilon)} = KE_{\text{obs}}^{\frac{i}{0}}(1 \pm 2\sigma_\epsilon) \tag{8}$$

where i is the index of the comparison station. The relative error associated with the ratio of two KE values was computed as the additive combination of their individual standard relative errors, as in (8) [17]. Here, σ_ϵ is the relative error for a desired confidence interval.

III. RESULTS

In June, 2011, a station-keeping survey with five stations (A–E, shown in Fig. 1) was conducted near Admiralty Head in Admiralty Inlet. Each station was occupied six times for 5 min, with an interval of 30–40 min between observations of the same station. The survey was conducted during a lesser ebb tide in the transitional period of the neap/spring cycle with peak current velocities around 2 m/s.

A. Station Comparison

The data collected from the shipboard ADCP were processed and analyzed as described in Section II. The hydrokinetic resource was compared among stations in Fig. 3, with station A taken as the reference station.

These results suggest that stations C, D, and E are the most energetic. This is especially evident in the lower bins where the relative KE is more than 10% higher at these target stations relative to the reference station.

B. Comparison Between Bottom-Mounted and Shipboard Data

Stations A, B, and C were chosen because these were cospatial with bottom-mounted ADCPs, allowing us to ground truth the effectiveness of the station-keeping survey methodology. A comparison of shipboard and bottom-mounted observations is

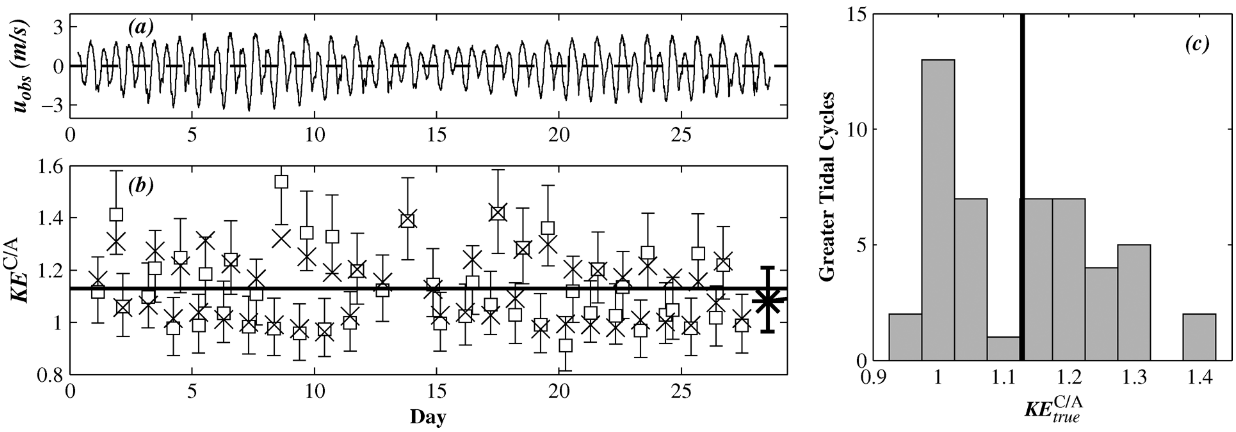

Fig. 5. Normalized KE values over multiple tidal cycles. Observations at 22-m elevation relative to the seabed. (a) Velocity observations at station C from bottom-mounted ADCP data. Dashed line separates flood cycles (positive velocities) and ebb cycles (negative velocities). (b) Normalized KE values (station C referenced to station A). X's denote "true" values. Squares denote observed values, with the error bars bounding the 68% confidence interval [set by the standard error (see Fig. 12)]. Horizontal line denotes the mean of the 48 true values, and star denotes the observed value during the June 2011 station-keeping survey. (c) Histogram of true normalized KE values. Vertical line denotes the mean of the 48 true values.

shown in Fig. 4. For this comparison, undecimated cotemporal bottom-mounted data were taken as "truth."

These results indicate good agreement between estimates for the kinetic energy density obtained from the shipboard and bottom-mounted observations. The error associated with KE values obtained in the upper half of the water column is within the expected error ($\sigma_\epsilon < 10\%$; Fig. 12). All bins of stations B and C are also within this expected error. The discrepancy in the observations in the lower bins at station A is attributable to an instrumentation configuration problem with the bottom-mounted ADCP.[2]

The normalized KE values ($KE^{i/0}$) for each station are shown in Table III. This table compares the results from station keeping to the true values for one tidal cycle derived from bottom-mounted data. The relative resource intensity observed from the two survey techniques yields similar results for this tidal cycle (e.g., the variation in resource intensity between stations A, B, and C is not statistically significant). In other words, for this tidal cycle, the estimates for relative resource intensity obtained from sparsely sampled vessel-based data are not statistically different from the estimate for relative differences obtained from continuous bottom-mounted data.

IV. Discussion

A. Ability to Resolve Long-Term Average Resource Variations

Based on the success of this method for a single tidal cycle, the effectiveness of the technique depends on two additional questions. First, will a station-keeping survey methodology identify the same relative differences as a grid of continuously sampling bottom-mounted profilers over all tidal cycles (i.e., is this result typical or random chance)? Second, how many tidal cycles must be observed using this methodology to identify long-term average variations in relative resource intensity?

The 30 days of simultaneous bottom-mounted data from stations A and C (sites 1 and 3, respectively) were partitioned into individual tidal cycles, of which 48 greater tidal cycles met the decimation analysis criteria (Section II-B). To mimic multiple station-keeping surveys at these locations, the true normalized KE value and the observed normalized KE value were computed from bottom-mounted data. The "true" value for normalized KE (i.e., $KE^{C/A}_{\mathrm{true}}$) for each tidal cycle was computed from the undecimated KE ensembles for a 2-h integration window around cycle peak. The corresponding observed value (i.e., $KE^{C/A}_{\mathrm{obs}}$) was calculated from the decimated realization for that cycle with a survey start time 90 min before peak currents. A comparison of these $KE^{C/A}$ values is shown in Fig. 5. Of the 48 greater tidal cycles, 47 of $KE^{C/A}_{\mathrm{true}}$ fall within the 68% confidence interval for $KE^{C/A}_{\mathrm{obs}}$, and all of the true values fall within the 95% confidence interval for observed values (not shown). As found in the June 2011 station-keeping survey, these results suggest that station C is, on average, somewhat more energetic than station A (see Fig. 3), though not statistically so. By coincidence, the best estimate from the station-keeping survey on this date falls quite close to the long-term average resource differences between these stations.

Although the station-keeping methodology generally performs well for a single tidal cycle [x's and squares compare well in Fig. 5(b)], the observed spatial resource differences vary with tidal cycle (i.e., the observed differences over a single survey is not likely to accurately represent the true long-term average relative differences). Therefore, we investigated the effectiveness of multiple station-keeping surveys over successive tidal cycles to improve the confidence that observed values reflect the true, long-term values.

The normalized KE metric, computed from a single station-keeping survey, was used to compare the hydrokinetic resource between target stations. As described in [1], metrics

[2]The distance between pings (equivalent to the time delay) was insufficient to avoid interference between the incoming and outgoing pulse in these bins. The along-beam distance of approximately 132 m ($2 \times 60/\cos(25^\circ) = 132$ m in 60-m depth) was greater than the lag of 120 m by 12 m, and thus the surface reflection would interact with the next transmitted ping 12 m away from the transducer. Analysis of the along-beam velocities indicates destructive interference, with along-beam velocities approaching zero in these bins (not shown). This would explain the consistent overestimation in current velocity observations of the shipboard ADCP relative to the bottom-mounted ADCP at station A at these elevations.

TABLE IV
COMPARISON OF KE AND $\overline{K}$

Station	Station-Keeping		Bottom-Mounted Deployments [a]	
	$\overline{(KE^{i/0})^S}$ [b]	S (consecutive surveys)	$\overline{(\overline{K}^{i/0})^T}$ [c]	T (deployment duration, days)
A (“0”)	1.00 ± 0.04	4	1.00 ± 0.04	356
C	1.13 ± 0.04	4	1.13 ± 0.08	30

[a] Bottom-mounted deployments are cospatial with station-keeping targets (Table II)
[b] Standard error with respect to 48-observation mean value (Fig. 5)
[c] Standard error with respect to its epoch value based on the analysis of harmonic currents [1]

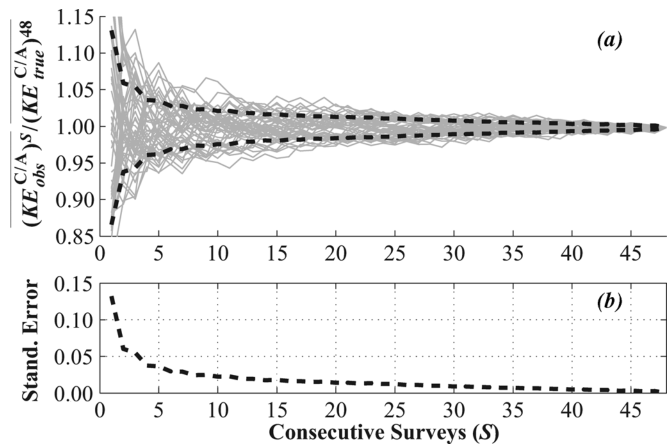

Fig. 6. Convergence of normalized KE to its long-term average. (a) Convergence to 48-observation mean value. Thin lines denote individual realizations over the 30-day period. Dashed lines denote standard error. (b) Standard error normalized by running mean normalized kinetic energy density as a function of observation time.

calculated from finite-length observations may diverge from their true values (defined as the average over an infinite observation). The convergence of the normalized KE metric to its true value is given by

$$\frac{\int_0^S KE^{C/A}(s)ds / \int_0^S ds}{\int_0^\infty KE^{C/A}(s)ds / \int_0^\infty ds} \tag{9}$$

where $KE^{C/A}(s)$ is the observed relative KE metric and S is the number of consecutive surveys. In shorthand, the averaging number of observations is represented with a superscript, and this is said to have converged to the long-term average when $\left(KE^{C/A}\right)^S \approx \left(KE^{C/A}\right)^\infty$. Since $\left(KE^{C/A}\right)^\infty$ is not known *a priori*, this convergence could only be investigated in a proximate manner. The true long-term average of the greater tidal cycles over an infinite number of observation $\left(KE^{C/A}\right)^\infty$ was approximated by the mean of the true normalized KE values obtained from the 48 tidal cycles meeting the survey criteria (Section IV-C) over the 30 days of mimicked station-keeping observations $\left(KE^{C/A}\right)^{48}$. Multiple 48-cycle realizations were created by generating a ring buffer from the 30-day data set. Fig. 6 shows the convergence of the normalized KE (station C referenced to station A), to its 48-observation mean value.

The normalized standard error relative to the long-term average decreases to less than 5% after four surveys on consecutive greater tidal cycles meeting the decimation analysis criteria (cycle duration, timing restrictions, current amplitude, as discussed in Section IV-C). The standard error then continues a gradual decay. Provided that data collection is performed as suggested in Section II (e.g., an equal number of observations to either side of peak currents is ideal), convergence trends are not markedly different for variations in survey start time relative to peak currents.

For the purposes of characterizing differences in the hydrokinetic resource between two locations, a record length of four consecutive surveys on greater tidal cycles provides at least 5% accuracy. Additional surveys may be necessary if an individual greater tidal cycle does not allow sufficient time for the survey to be conducted or does not provide strong signal for resolving spatial variations (i.e., peak currents less than 1 m/s). The standard error for a single survey can approach 20%, which may be unacceptably high for optimizing subsequent deployment of a bottom lander to estimate turbine power generation.

A comparable metric to the KE for characterizing long-term average differences in the hydrokinetic resources from current velocity observations of bottom-mounted ADCPs is the mean kinetic power density—the time average of the kinetic power density—given by

$$\overline{K} = \overline{\frac{1}{2}\rho u_{\text{obs}}^3}. \tag{10}$$

Following from [1], this resource characteristic was computed for the bottom-mounted ADCP deployments at sites 1 and 3 (cospatial with stations A and C, respectively). The comparison of the normalized KE values $(KE^{i/0})$ from multiple station-keeping surveys (mimicked using the decimated data) and the normalized $\overline{K}$ values $(\overline{K}^{i/0})$ from the complete bottom-mounted data is shown in Table IV.

In summary, this vessel-based methodology is capable of capturing the same spatial trends in relative resource intensity as those developed from a grid of higher cost bottom-mounted deployments.

B. Impact of Positions Errors

As discussed in Section II-B, in order for observations between two stations to be statistically independent (2), the position ambiguities cannot overlap. This ambiguity establishes the smallest resolvable resource variations. The spatial separation necessary for this independence is governed by the positioning errors in the survey, namely the track error, DGPS uncertainty, and Doppler profiler beam spread that are uncorrelated and can be combined to obtain a total position error.

For the June 2011 station-keeping survey, the beam spread was approximately 31 m at a bin elevation of 22 m, and the track error was approximately 22 m for each station. From (1), this yields a total position error of 38 m associated with each station. Consequently, station B was not statistically independent from the reference (station A), as the locations were only separated by 52 m and their combined total position errors were 76 m (i.e., spatial overlap of 24 m). Of the pings collected during observations over these stations, approximately 20% overlapped with the station not being surveyed.

The resolution of the station-keeping methodology is limited by these positioning errors. The total position error defines the resolution radius associated with each station (i.e., the resolution is twice the total position error) and choosing target stations that are separated by at least twice the expected total position error improves survey effectiveness. Note that beam spread is a function of depth, resulting in a depth-dependent region of ambiguity, so it is possible for the observations from two stations to be statistically independent near the surface and not statistically independent at lower elevations relative to the seabed. Furthermore, tighter tolerances in the vessel's track about the target station reduce the spatial ambiguity and increase the possible resolution for a station-keeping survey.

C. Choice of Survey Parameters

The survey parameters recommended in Section II-B were chosen to maximize the quality of data collected. Here, a more detailed discussion is provided to justify the choice of temporal resolution, spatial resolution, tidal conditions during the survey, and observation timing.

1) Temporal Resolution: The duration of each station occupation was chosen to capture only information about the deterministic component of the currents by averaging out variability associated with Doppler noise and turbulent fluctuations. As seen in

$$u_{\mathrm{meas}} = u_{\mathrm{det}} + u_{\mathrm{met}} + u_{\mathrm{turb}} \pm n_{\mathrm{samp}} \qquad (11)$$

a single ADCP ping (u_{meas}) reflects not only the deterministic tidal forcing (u_{det}) and meteorological component (u_{met}), but also turbulence fluctuations (u_{turb}) and the Doppler noise from the instrument (η_{samp}). As stated in [1], the deterministic currents include harmonic currents, described by harmonic constituents [18], [19], as well as the aharmonic response to these currents induced by local topography and bathymetry. Aharmonic currents are not described by tidal constituents, but are repeatable, site-specific flow features [13]. Meteorological currents include wave- and wind-induced motion [20], [21], residual currents associated with estuarine stratification [22], and storm surges [23]. Turbulent currents include large-scale horizontal eddies and small-scale isotropic turbulence [15]. The relative contribution of these elements to measured currents is site specific.

To reduce the Doppler noise inherent to single-ping ADCP data, the data from shipboard surveys were aggregated into a series of volumetric bins. A certain number of samples were necessary in each bin to achieve some standard of normal statistics and the noise had to be reduced, but the number of samples had to be such that the deterministic and meteorological currents were statistically stationary and an assumption of vertical homogeneity within each sample bin was valid.

A vertical bin size of 4.0 m was selected for this application because it resulted in an acceptably low Doppler uncertainty per ping (0.05 m/s) and still provided information at a resolution sufficient for siting decisions. However, the implicit assumption of spatial homogeneity over the depth bins should be viewed with some caution, especially near the seabed where the velocity profile changes significantly with depth due to the influence of the boundary layer (Polagye and Thomson [1] provide further discussion on this point).

A canonical value for turbulence intensity over all stages of the tide (i.e., the turbulent velocity fluctuations relative to the mean tidal currents) is 10% [15]. Strong currents at potential tidal energy sites, including northern Admiralty Inlet, can exceed 3 m/s. It was assumed that both the Doppler noise and turbulence fluctuations are normally distributed about the mean, deterministic currents.

Reducing the contribution from turbulence and Doppler noise to the measured current velocity required a minimum number of sample pings per station occupation. The minimum sample size was determined using confidence intervals for a nonstandard normal distribution (12) and comparing them to the interval set by the desired precision (13)

$$u = u_{\mathrm{obs}} \pm Z_{(\alpha/2)} \frac{s}{\sqrt{N}} \qquad (12)$$

$$u = u_{\mathrm{true}} \pm p \qquad (13)$$

Here u is the estimated population mean, u_{true} is the true population mean (unknown), u_{obs} is the sample mean (ensemble average), Z is the normal inverse cumulative distribution, α is the confidence level, s is the sample standard deviation, N is sample size, and p is the desired precision.

The minimum number of required samples that yield the desired precision was determined by an estimate for the standard deviation (i.e., both Doppler noise and turbulence) and a confidence level. In other words, with the standard deviation set by Doppler noise and turbulence velocity fluctuations, and the normal inverse cumulative distribution set by the confidence level, the number of samples on the right-hand side of (12) was chosen such that the ensemble-average velocity confidence interval was less than or equal to the desired precision for the true velocity on the right-hand side of (13). To determine, *a priori*, the minimum number of samples required for the June 2011 station-keeping survey in Admiralty Inlet, the Doppler uncertainty was modeled as ±0.05 m/s (Table I), and the turbulence velocity fluctuations were modeled as ±0.30 m/s (10% of 3-m/s velocity). The relation between precision and sample size is shown in Fig. 7.

Greater precision requires increasing the number of samples per ensemble interval. For a station-keeping survey, it was desired that the measurement precision be significantly less than the spatial resource variations that are of operational interest for a tidal energy project developer. For the June 2011 survey, the desired precision was on the order of 0.10 m/s (i.e., a higher precision than could be obtained by the survey methodology described in [14]). At least 143 samples per ensemble interval were required to obtain 0.05-m/s precision. With the configuration shown in Table I, the ADCP received a good ping every 1–2 s and 5-min ensembles yielded better than 0.05-m/s precision. In [15], 5-min ensembles were empirically determined to be the longest duration with a stable mean and variance (i.e., stationary

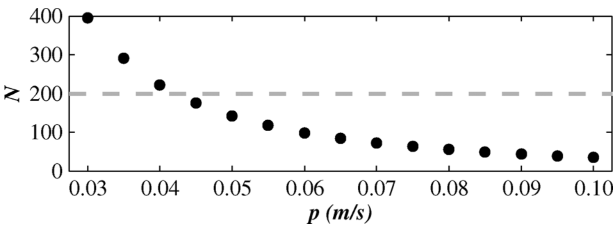

Fig. 7. Sample size requirements for the June 2011 survey. Normal statistics with 95% confidence for Doppler uncertainty in Table I and turbulence consistent with observations from Admiralty Inlet. Dashed line denotes the number of samples from a 5-min observation receiving good pings every 1–2 s.

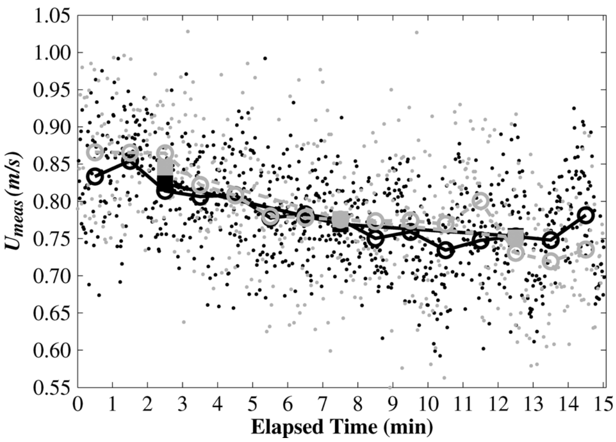

Fig. 8. Shipboard and bottom-mounted ADCP velocity observations. Raw and ensemble-averaged observations at 22-m elevation relative to seabed at station C. Black dots denote bottom-mounted pings, and gray dots denote shipboard pings. Bottom-mounted ensembles are connected by solid lines, and shipboard ensembles are connected by dashed lines. Circles denote 1-min ensemble intervals, and squares denote 5-min ensemble intervals.

statistics) that was insensitive to the detrending scheme, while windows shorter than 5 min tended to be influenced by turbulence.

To confirm the observation duration was sufficient to achieve the desired precision, a single extended observation was conducted at Station C before the start of the June 2011 survey. As shown in Fig. 8, the observations from the shipboard ADCP are ensembled over different intervals and compared to cotemporal and cospatial bottom-mounted data. The 5-min ensemble interval captures the trend in the deterministic components of the current magnitude, with minimal fluctuations. In addition, over this interval, the difference between shipboard observations and bottom-mounted "truth" is small in comparison with the desired precision.

2) Spatial Resolution: For the June 2011 survey, the 50-m tolerance radius around the target station for the vessel was selected *a posteriori* as this was the minimum tolerance that could be achieved by the *R/V Jack Robertson*'s captain in strong and variable currents. Vessels equipped with dynamic positioning systems may be able to achieve tighter tolerances.

DGPS coordinate location (converted to relative easting x and northing y, with respect to the reference station) was recorded for each ADCP ping (GPS mast was almost directly above the ADCP wet well). For the series of observations at an individual station, the target location became the mean of the ping locations, rather than the original target location, to better characterize the accuracy of the collected data. The track error (δ_{track}) was computed as the mean distance from the ping locations to mean survey position. The coordinate error associated with the use of a DGPS (δ_{DGPS}) was minimal and assumed to be no more than 5 m. This error could be significant if a station-keeping survey was to be conducted without a DGPS. Doppler profiler beam spread is defined as $\delta_{\mathrm{beam}} = 2d\tan(\theta)$, where θ is the transducer mounting angle from vertical and d is the vertical distance between the transducer head and sample bin. For a shipboard measurement, beam spreading is small near the surface, and it is reasonable to assume that spatial homogeneity is achieved between the beams (four beams in this specific case). As shown in Fig. 2, this assumption becomes more tenuous at greater depths, particularly when attempting to resolve small spatial scales. The cross section of the horizontal area being surveyed was considered the beam spread error.

3) Tidal Conditions: To evaluate the ability of the station-keeping methodology to consistently rank resource intensity between locations, bottom-mounted data were decimated to mimic shipboard data. To simulate a survey pattern, six sequential ensembles, each separated by 35 min, were selected. Because the timing of peak currents may not be known, in advance, to high accuracy, variations in observation timing relative to peak currents were considered. By incrementing the starting time for each survey, each decimated bottom-mounted data set yielded 20 survey realizations per tidal cycle that contained at least two observations on each side of peak currents (i.e., two observations before peak and four after or *vice versa*). To obtain these realizations, a tidal cycle needed to be at least 4.5 h in duration, with peak currents occurring at least 2.25 h after and before slack water. Tidal cycles that pass the criteria allow sufficient time for the survey to be conducted (with some flexibility in survey start time relative to peak currents) and provide strong signal for resolving spatial variations. Applying the decimation analysis criteria (timing restrictions, current amplitude) to the annual data set provided insight into the tidal conditions in which station-keeping surveys are effective. Each tidal cycle in the decimated data set was categorized by the direction (flood/ebb), diurnal inequality (greater/lesser), and fortnightly variation (spring/neap). A comparison of the pass rates for the categories of tidal conditions in Admiralty Inlet is shown in Fig. 9. Of the 1345 tidal cycles observed by the bottom-mounted ADCP at site 1, 849 satisfied the above criteria.

Whether an individual tidal cycle passes the analysis criteria is primarily influenced by diurnal inequality, and appears to be independent of the direction (i.e., ebb versus flood) and fortnightly variation. Note that the diurnal inequality is a feature of mixed tidal regimes, such as occur along most of the west coast of the United States. The duration of the lesser tides of the diurnal inequality is often too short or low intensity for a station-keeping survey. These results suggest that in locations of mixed tidal regimes, the effectiveness of station-keeping surveys is improved when they are performed during greater tides, which provide strong signal and enough time for all six observations to be collected. Surveys on lesser tides in the transition between neap and spring may also be suitable for surveying as, in some cases at this specific location, the greater and lesser tides during this period may be nearly equal in strength.

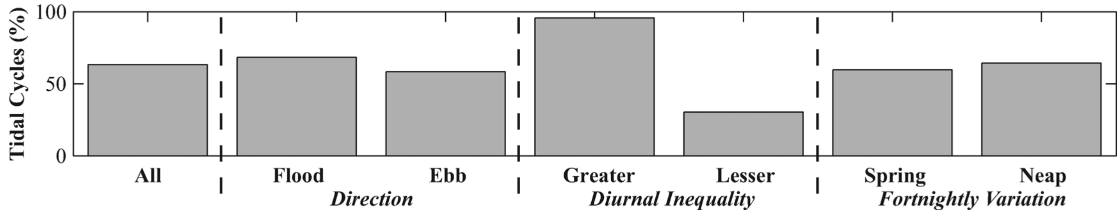

Fig. 9. Decimation analysis on tidal conditions. Percentages of tidal cycles satisfy the decimation analysis criteria (1-m/s peak currents, 4.5-h cycle duration, peak currents occurring at least 2.25 h after and before slack water).

4) Observation Timing: Using the kinetic energy density metric and the standard relative error in its computation, perturbations to the baseline observation parameters (i.e., six observations per station with temporal spacing of 35 min) were considered using the decimated data set. The objective was to choose a number of observations and time between observations that minimized σ_ϵ. The number of realizations per tidal cycle for each of the cycles in the decimated data set depends on the observation parameters being analyzed (i.e., number of observations and temporal spacing between observations). For all realizations of the station-keeping survey scenarios analyzed, the difference between the number of observations collected before peak currents and the number of observation collected after peak currents was never greater than two. The standard relative error for each scenario was found as the mean of the relative errors for all realizations. Results of this analysis are shown in Fig. 10.

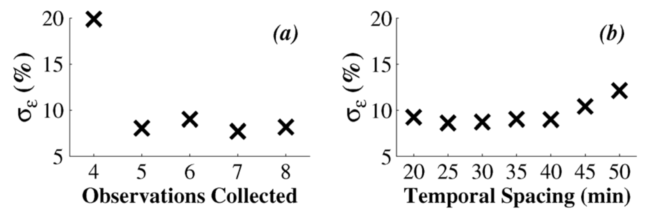

Fig. 10. Effects of varying survey parameters on computation of KE. (a) Effect of varying number of observations collected with time between observations held constant at 35 min. (b) Effect of varying time between observations with the number of observations held constant at six. Both analyses performed at 22-m elevation relative to the seabed.

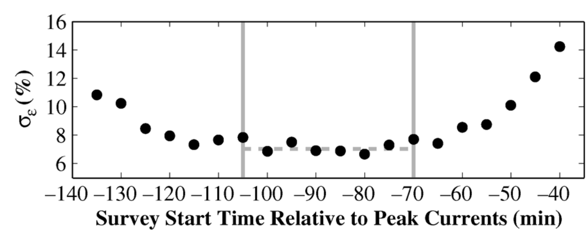

Fig. 11. KE standard error based on survey start time relative to peak currents. Circles denote standard relative error for each survey start time. Solid lines denote conservative start time bounds for which an equal number of observations are collected on either side of peak (six stations, 35-min separation between observations at each station). Dashed line denotes the standard relative error for survey start times within these bounds. Analyses performed at 22-m elevation relative to seabed.

These results demonstrate that collecting at least five observations per station substantially decreases the standard relative error in the computation of the KE. The temporal spacing between observations also influences the computation of the KE. The 2-h KE value bracketing peak currents is of primary interest, and smaller spacing (e.g., 20–25 min) between observations can result in a better estimate of the KE because of the higher resolution during this window. However, high σ_ϵ can result from such a station-keeping survey if observations occur primarily to one side of peak currents (not shown) because one of the ends of the window is not well bounded for curve fitting. Longer intervals between observations at the same station (e.g., 45–50 min) result in lower resolution around peak currents, provide less flexibility in survey start time, and increase the overall duration of the survey. Collecting observations with temporal spacing of 30–40 min provides sufficient resolution around peak currents, does not necessitate an entirely equal number of observations on each side of peak currents, and, therefore, allows flexibility in survey start time relative to the timing of peak currents. Therefore, the recommended survey strategy is to bracket peak currents at all stations and occupy each station at least five times, with a 30–40-min interval between each occupation of the same station.

The effect of starting time relative to peak currents was also evaluated. The standard relative error for each survey start time shown in Fig. 11 was computed as the mean of the relative errors of that set of realizations. Realizations with start times that include an equal number of observations on both sides of the peak have the smallest relative errors. This indicates that the effectiveness of a station-keeping survey is improved when the survey starts approximately 70–105 min before the time of peak currents. Given that the time of peak currents may not be known to high accuracy before the survey is initiated (and may vary by more than 60 min between the surface and seabed), conservative start times are indicated. Assuming that the survey begins as discussed, the standard relative error was calculated as the mean of all realizations meeting these criteria.

Fig. 12 shows the distribution of relative errors for one vertical bin and the standard relative error throughout the water column. The distribution of these errors has a nearly zero mean value indicating that the data processing techniques did not bias the computation of the KE. The 2-h period was thus a reasonable choice for the integration window. Testing with other windows indicated that periods less than 2 h or more than 3 h tend to introduce a systematic error in the computation of the KE (i.e., nonzero mean value for ϵ).

Furthermore, these results suggest that the station-keeping survey methodology can be improved by surveying during greater tidal cycles, which is demonstrated in the comparison of the standard relative error values between all tidal cycles and greater tidal cycles [Fig. 12(b)]. Velocity varies less smoothly

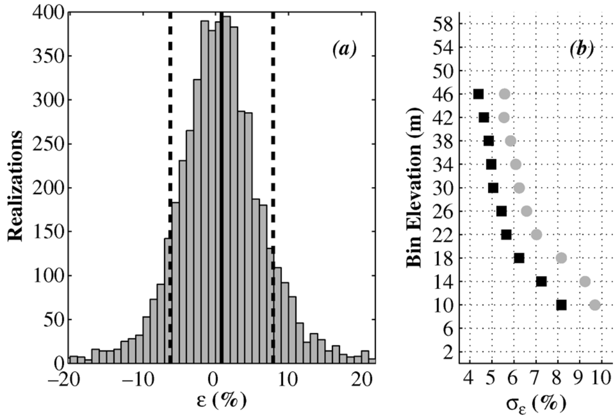

Fig. 12. KE standard relative error for conservative start times. (a) Distribution of error at 22-m elevation relative to seabed. Solid line denotes mean value, and dashed lines denote one standard deviation from the mean value. Three standard deviations from the mean value of the distribution are shown. (b) KE standard relative error throughout water column. Circles denote the standard relative error for all tidal cycles, and squares denote the standard relative error for greater tidal cycles.

in time near the seabed due to the influence of bottom effects (bottom friction and local acceleration due to bathymetry). The standard error, as calculated relative to the undecimated observations of K, increases near the seabed. We suspect that this is a data processing artifact associated with the increasingly complex variations in current intensity near the seabed (i.e., the second-order polynomial fit may not describe the currents near the seabed as well as it does closer to midwater).

D. Cost Considerations

A grid of bottom-mounted ADCPs provides simultaneous stationary measurements with low uncertainty, but as demonstrated in Section IV-A, performing the vessel-based station-keeping methodology during multiple, consecutive greater tidal cycles captures the same spatial trends as those characterized by a long-term deployment of a grid of bottom-mounted profilers.

For a bottom-mounted grid, deployment and recovery operations can only take place around slack water, and the number of instrumentation packages that can be deployed or recovered per slack is dependent on slack duration and tidal conditions. Deploying or recovering several instrumentation packages would likely require at least two slack waters, and a day of ship time on an appropriate vessel (i.e., equipped with an A-frame, winch, load-bearing acoustical release, command/ranging deck unit) would be allocated on each end of deployment for this purpose. Additionally, this approach would incur the expense of each instrumentation package (i.e., ADCP, frame, ballast, acoustical release, float) as well as technician time to mobilize and demobilize the packages.

Performing the vessel-based station-keeping methodology to achieve 5% accuracy in capturing the same spatial differences as those characterized by the bottom-mounted deployments requires a record length of four consecutive surveys on greater tidal cycles, equivalent to two days of ship time on an appropriate vessel (i.e., equipped with an ADCP and capable of holding station in strong currents).

Fully burdened ship time and instrumentation package costs will be dependent on the availability of these resources. Nonetheless, each approach has a base cost of two days of ship time, with the bottom-mounted grid incurring the additional expense of the instrumentation packages. Therefore, the station-keeping methodology is an economically favorable option for resource mapping for the purpose of generating siting data. Once relative variations in the tidal resource intensity have been established, a long-term (i.e., 30 day) bottom deployment is still necessary to assess the absolute resource intensity and other relevant characteristics (e.g., quantification of turbulence, directional variability).

V. Conclusion

A vessel-based survey methodology is presented that is suitable for resolving small spatial scale differences and minimizing uncertainty in results. Spatial resolution of 100 m or less is possible by selecting stations such that their spatial ambiguities do not overlap, and the resolution could be further improved by tighter tolerances in the vessel's track about the target station. Uncertainty in the results is minimized by determining a minimum duration of each station occupation that filters turbulence and Doppler uncertainty from ensemble averages.

Analysis of a yearlong bottom-mounted ADCP data set indicates the most effective tidal conditions to conduct the survey, determines optimal observation timing and spacing, and reduces the potential for data processing artifacts (i.e., sensitivity to type of fit). Bottom-mounted data sets were also used as "truth" to evaluate the accuracy of the methodology and its effectiveness. Results indicate good agreement between shipboard and bottom-mounted observations in capturing spatial trends of the hydrokinetic resource over a single tidal peak. Multiple, consecutive observations during greater tidal cycles can be used to characterize relative resource variations with accuracy approaching long-term (i.e., 30 day) bottom-mounted deployments.

Station keeping is an effective and economically favorable alternative to generating siting data from a high-resolution grid of bottom-mounted ADCPs.

Appendix
Choice of Fitting Technique

Three types of empirical fits were considered to represent the resource intensity. The first was a polynomial fit

$$\widetilde{K}(t) = x_0 + x_1 t + \dots x_n t^n \tag{14}$$

where $\widetilde{K}$ is the empirical fit to the observations of K and x are the polynomial coefficients. The second was a modified polynomial fit where the coefficients were determined by bottom-mounted ADCP data obtained simultaneously with the shipboard data at one location within the survey area. This was a hybrid survey technique that combined aspects of shipboard and bottom-mounted surveys methodology. An amplitude correction factor and time offset became the free parameters being fit at each station and depth. This enabled the use of higher order

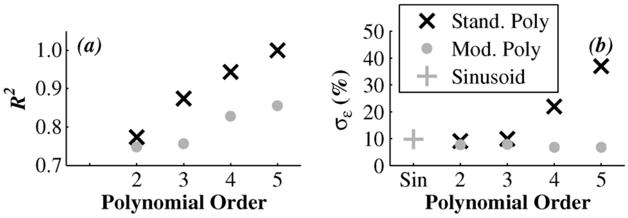

Fig. 13. Quality of fits to K. (a) Goodness of fit to observed data. Note that the sinusoid fit is not shown because R^2 value is not comparable to the other fits (i.e., for the sinusoid fit, the fit is applied to the velocity ensembles and the result is then cubed, whereas for the second-order polynomial fit, the fit is applied directly to the kinetic power density). (b) Quality of fit in calculating KE. Both analyses performed at 22-m elevation relative to seabed.

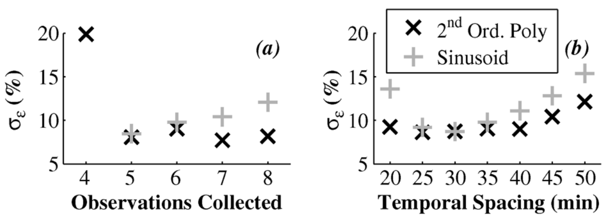

Fig. 14. Effects of varying survey parameters on computation of KE. (a) Effect of varying number of observations collected with time between observations held constant at 35 min. (b) Effect of varying time between observations with the number of observations held constant at six. Both analyses performed at 22-m elevation relative to the seabed.

polynomials to describe the time variation in K. The third was a sinusoid fit, similar to the one used by Epler *et al.* [14]

$$\widetilde{K}(t) = \frac{1}{2}\rho\left(A\sin(\omega t + \phi)\right)^3 \tag{15}$$

where A is the current velocity amplitude, ω is the tidal cycle frequency, and ϕ is the relative phase. While this fit had some justification on the basis of harmonic analysis, measured tidal currents at tidal energy sites rarely resemble a smoothly varying sinusoid [13]. The decimated data set was used to benchmark the effectiveness of these three possible fits. Results are shown in Fig. 13, and the quality of the various fits is discussed as it pertains to the kinetic energy density.

The KE associated with each of the potential curve fits was calculated for all tidal cycle realizations in the decimated data set ($N = 849$ tidal cycles with 20 realizations per cycle). For each of the fit types, a standard relative error (σ_ϵ) was defined as the standard deviation of the relative errors for all realizations. A comparison of the quality of fits is shown in Fig. 13.

For the basic polynomial fits, increasing the order of the polynomial improves the coefficient of determination. However, higher order fits are prone to buckling and do not necessarily represent the underlying structure of the data accurately. This is evident in the high relative errors associated with the fifth-order fit (even though the coefficient of determination is highest). The second-order polynomial and sinusoid descriptions of the kinetic energy density perform nearly as well as all orders of the modified polynomial informed by bottom-mounted data. The minimal improvement gained by using bottom-mounted data to inform the fitting is not justifiable because of the higher execution cost to deploy and recover autonomous bottom-lander equipment simultaneously with shipboard surveys. A comparison between the second-order polynomial and sinusoid descriptions indicates that they perform similarly throughout the water column (not shown). The effectiveness of these fits was further tested in the context of the observation parameters. Results of this analysis are shown in Fig. 14.

The second-order polynomial and sinusoid fits again perform similarly for sampling intervals around the baseline parameters (i.e., six observations separated by 35 min). In scenarios nearing the limits of the variations applied to the observation parameters, the second-order fit appears to be more accurate. Particularly for the scenario of four observations in Fig. 14(a) the σ_ϵ value is approximately 63% for the sinusoid fit (not shown) and only 20% for the second-order polynomial fit. The second-order polynomial fit proves to be more robust in representing the underlying data with variations to these observation parameters. As such, it was used to represent the resource intensity in all previous discussion.

ACKNOWLEDGMENT

The authors would like to thank J. Talbert, A. de Klerk, C. Bassett, and Capt. A. Reay-Ellers for their assistance in collecting these data.

REFERENCES

[1] B. Polagye and J. Thomson, "Tidal energy resource characterization: Methodology and field study in Admiralty Inlet, Puget Sound, US," *Proc. IMechE A, J. Power Energy*, to be published.

[2] J. Simpson, E. Mitchelson-Jacob, and A. Hill, "Flow structure in a channel from an acoustic Doppler current profiler," *Continental Shelf Res.*, vol. 10, no. 6, pp. 589–603, 1990.

[3] R. Proctor and J. Wolfe, "An investigation of the storm surge of 1st February 1983 using numerical models," *Focus Model. Mar. Syst.*, vol. 1, pp. 43–72, 1990.

[4] W. Geyer and R. Signell, "Measurements of tidal flow around a headland with a shipboard acoustic Doppler current profiler," *J. Geophys. Res.*, vol. 95, no. C3, pp. 3189–3197, 1990.

[5] R. Vennell, "Acoustic Doppler current profiler measurements of tidal phase and amplitude in Cook Strait, New Zealand," *Continental Shelf Res.*, vol. 14, no. 4, pp. 353–364, 1994.

[6] R. Vennell and N. Collins, "Acoustic Doppler current profiler measurements of tides in Cook Strait, New Zealand," in *Proc. 10th Australasian Conf. Coastal Ocean Eng.*, 1991, no. 21, pp. 529–534.

[7] J. Candela, R. Beardsley, and R. Limeburner, "Removing tides from ship-mounted ADCP data, with application to the Yellow Sea," in *Proc. IEEE 4th Working Conf. Current Meas.*, April 1990, pp. 258–266.

[8] M. Foreman and H. Freeland, "A comparison of techniques for tide removal from ship-mounted acoustic Doppler measurements along the southwest coast of Vancouver Island," *J. Geophys. Res.*, vol. 96, no. C9, pp. 17 007–17 021, 1991.

[9] A. Münchow, R. Garvine, and T. Pfeiffer, "Subtidal currents from a shipboard acoustic Doppler current profiler in tidally dominated waters," *Continental Shelf Res.*, vol. 12, no. 4, pp. 499–515, 1992.

[10] M. Cáceres, A. Valle-Levinson, and L. Atkinson, "Observations of cross-channel structure of flow in an energetic tidal channel," *J. Geophys. Res.*, vol. 108, no. C4, pp. 1–10, Apr. 2003.

[11] C. Stevens, M. Smith, B. Grant, C. Stewart, and T. Divett, "Tidal energy resource complexity in a large strait: The Karori rip, Cook Strait," *Continental Shelf Res.*, vol. 33, pp. 100–109, 2012.

[12] R. Vennell and R. Beatson, "Moving vessel acoustic Doppler current profiler measurement of tidal stream function using radial basis functions," *J. Geophys. Res.*, vol. 111, no. C9, pp. 1–15, Sep. 2006.

[13] B. Polagye, J. Epler, and J. Thomson, "Limits to the predictability of tidal current energy," in *Proc. OCEANS Conf.*, Sep. 2010, DOI: 10.1109/OCEANS.2010.5664588.

[14] J. Epler, B. Polagye, and J. Thomson, "Shipboard acoustic Doppler current profiler surveys to assess tidal current resources," in *Proc. OCEANS Conf.*, Sep. 2010, DOI: 10.1109/OCEANS.2010.5664387.

[15] J. Thomson, B. Polagye, V. Durgesh, and M. Richmond, "Measurements of turbulence at two tidal energy sites in Puget Sound, WA," *J. Ocean. Eng.*, vol. 37, no. 3, pp. 363–374, Jul. 2012.
[16] Teledyne RD Instruments, "Acoustic Doppler current profiler principles of operation: A practical primer," Poway, CA, RDI P/N 951-6069-00, 2006.
[17] J. Taylor, *An Introduction to Error Analysis: The Study of Uncertainties in Physical Measurements*, ser. Books in Physics. Sausalito, CA: University Science Books, 1982, ch. 3.
[18] G. Godin, "On the predictability of currents," *Int. Hydrograph. Rev.*, vol. 60, pp. 119–126, 1983.
[19] M. Foreman, R. Crawford, and W. Marsden, "De-tiding: Theory and practice," *Quant. Skill Assessment Coastal Ocean Models, Coastal Estuarine Studies*, vol. 47, pp. 203–239, 1995.
[20] D. Wang, "Wind-driven circulation in the Chesapeake Bay, winter, 1975," *J. Phys. Oceanogr.*, vol. 9, no. 3, pp. 564–572, May 1979.
[21] C. Mei, *The Applied Dynamics of Ocean Surface Waves*, ser. Ocean Engineering. Singapore: World Scientific, 1989, ch. 1.
[22] D. Hansen and M. Rattray, "Gravitational circulation in straits and estuaries," Sears Found. Mar. Res., Dept. Oceanogr., Univ. Washington, Seattle, WA, Tech. Rep., 1965.
[23] D. Pugh, *Tides, Surges, and Mean Sea-Level*. New York: Wiley, 1987, ch. 6.

Michael Palodichuk received the B.S. degree in mechanical engineering from Gonzaga University, Spokane, WA, in 2010 and the M.S. degree in mechanical engineering from the University of Washington, Seattle, in 2012.

As a Graduate Research Aassistant at the University of Washington, he was a member of the Northwest National Marine Renewable Energy Center and the Applied Physics Laboratory. He now consults for the marine energy industry.

Brian Polagye received the B.S.E. degree in mechanical engineering from Princeton University, Princeton, NJ, in 2000 and the Ph.D. degree in mechanical engineering from the University of Washington, Seattle, in 2009.

Since 2009, he has been a faculty member in the Department of Mechanical Engineering, University of Washington, and since 2011, the Co-Director of the Northwest National Marine Renewable Energy Center. His research interest is marine renewable energy, including resource characterization, environmental effects, and micropower for instrumentation.

Jim Thomson received the Ph.D. degree in applied ocean physics from the Massachusetts Institute of Technology/Woods Hole Oceanographic Institution joint program, Woods Hole, MA, in 2006.

Later that same year, he joined the Applied Physics Laboratory, University of Washington, Seattle. In 2009, he began a joint appointment in the Faculty of Civil & Environmental Engineering, where he teaches fluid mechanics and coastal engineering. His research program includes basic and applied ocean research, with an emphasis on field measurements of waves and currents. As a member of the Northwest National Marine Renewable Energy Center, he is applying these techniques to characterize sites for marine energy development.